



# Survival of the Qaidam Mega-Lake System under Mid-Pliocene Climates and its Restoration under Future Climates

Dieter Scherer<sup>1</sup>

<sup>1</sup> Chair of Climatology, Technische Universität Berlin, Berlin, 12165, Germany

5 *Correspondence to:* Dieter Scherer (dieter.scherer@tu-berlin.de)

**Abstract.** The Qaidam basin in the north of the Tibetan Plateau, has undergone drastic environmental changes during the last millions of years. During the Pliocene, the basin contained a freshwater mega-lake system although the surrounding regions showed increasingly arid climates. With the onset of the Pleistocene glaciations, lakes began to shrink, and finally disappeared almost completely. Today, hyperarid climate conditions prevail in the low-altitude parts of the basin. The question, how the lake system was able to withstand the regional trend of aridification for millions of years, remained enigmatic, so far. This study reveals that the mean water balance of the basin is nearly zero under present climate conditions, and positive during warmer, less dry years. This finding provides a physically based explanation, how mid-Pliocene climates could sustain the mega-lake system, and that near-future climates not much different from present conditions could cause rising lake levels and expanding lake areas, and may result in restoration of the Qaidam mega-lake system over geological time scales. The study reveals that a region discussed as being an analogue to Mars due to its hyperarid environments is at a tipping point under present climate conditions, and may switch from negative values that have prevailed during the last 2.6 million years to positive ones in the near future.

## 1 Introduction

Paleogeographic studies (Chen and Bowler, 1986; Huang et al, 1993; Mischke et al., 2010; Wang et al., 2012) on the intermontane endorheic Qaidam basin, located in China's desert region north of the Tibetan Plateau (TP), revealed that it once contained a freshwater mega-lake system of ca. 120,000 km<sup>2</sup> lake surface during the mid-Pliocene (ca. 3.3-3.0 Ma BP). The onset of the Pleistocene glaciations at ca. 2.6 Ma BP marked a period of increased variability of climate, lake level and extent, as well as changes in salinity (Huang et al, 1993; Wang et al., 2012; An et al., 2001; Heermance et al., 2013). The mega-lake system finally disappeared during the last 100 ka (Madsen et al., 2014; Yu et al., 2019). Today, only few saline lakes and playas exist, and the low-altitude parts of the basin are hyper-arid deserts (Chen and Bowler, 1986; Huang et al, 1993; Wang et al., 2012). Paleoclimate studies (An et al., 2001; Miao et al., 2013) could prove that climates in the region have become increasingly dry throughout the Pliocene. However, the existence of a mega-lake system during this period implies that long-term mean annual water balance  $\Delta S$ , i.e., the total change in water storage within the basin's reservoirs, was zero or even



positive, and did not show, on average, negative values over time periods of thousands of years or longer, because otherwise, the mega-lake system would have temporarily dried out and produced layers of evaporites.

The water balance equation of a drainage basin is given by

$$\Delta S = P - ET + \Delta Q_{sfc} + \Delta Q_{sub}, \quad (1)$$

where  $P$  is precipitation,  $ET$  is actual evapotranspiration, while  $\Delta Q_{sfc}$  and  $\Delta Q_{gw}$  are net influx of surface and ground water into the basin. For endorheic basins  $\Delta Q_{sfc}$  is zero by definition. Groundwater entering or leaving a basin is generally difficult to quantify but can be neglected for the water balance of large intermontane basins like the Qaidam basin, which extends over ca. 254,000 km<sup>2</sup>. Thus,  $\Delta S$  of the Qaidam basin can be approximated by

$$\Delta S = P - ET. \quad (2)$$

The term  $P - ET$  is also referred to as net precipitation (Morrow et al., 2011), effective precipitation (Pritchard et al., 2019), or water availability (Greve et al., 2018), which is particularly relevant for studies of river basins where  $\Delta Q_{sfc}$  is generally negative, and thus  $P - ET$  is not equal to the water balance.

This study addresses the question how mean annual water balance in the Qaidam basin could have been zero or even positive over millions of years under very dry climates. I hypothesise that the high mountain ranges in the Qaidam basin receive sufficient precipitation such that very low amounts of precipitation at lower altitudes and water losses by actual evapotranspiration are compensated when both physical quantities are spatially averaged over the basin's entire area. This study does, however, not intend to reconstruct the climates of the past. Moreover, a physically based explanation for the long-term existence of the mega-lake system under dry climate conditions is sought. Since the mid-Pliocene is often regarded as past analogue for modern climate changes (Zubakov and Borzenkova, 1988; Haywood et al., 2016), this study also intends to provide a rational basis for assessing environmental changes that might be caused by climate changes as projected in this region for the future (Burke et al., 2018; Gu et al., 2018; Hui et al., 2018).

## 2 Data and methods

Fig. 1 provides an overview on the Qaidam basin and its surrounding regions in the north of the TP. The boundary of the Qaidam basin was delineated by Lehner and Grill (2013) from a digital elevation model (DEM) derived from data of the Shuttle Radar Topography Mission (SRTM).

### 2.1 Meteorological data from the High Asia Refined analysis

Meteorological data for 14 hydrological years (2001-2014) covering the period from 10/2000 to 09/2014 were taken from the first version (V1) of the High Asia Refined analysis (HAR) data set (Maussion et al., 2011; 20) for the model domain of 10 km grid spacing. In High Asia, hydrological years start in October, and are numbered by the calendar year to which January belongs (i.e., the hydrological year 2001 starts in October 2000). The HAR V1 data set was produced by dynamical downscaling of global gridded atmospheric data of the National Centers for Environmental Prediction (NCEP) Operational



60 Model Global Tropospheric Analyses (FNL) with the Weather Research and Forecasting (WRF) model version 3.3.1 to two  
regional domains of 30 km and 10 km grid spacing as described by Maussion et al. (2011) and 20. In contrast to regional  
climate simulations, the WRF model is re-initialised every day, and integrated only over 36 hours. Data of the first twelve  
hours are discarded to avoid artefacts eventually caused by model spin-up. The resulting data covering a full day are thus  
strongly constrained by the observed large-scale state of the atmosphere. Temporal resolution of the HAR V1 10 km data set  
65 is one hour. HAR V1 data used in this study were aggregated to monthly values. Monthly data for air temperature  $T$  (2 m above  
ground) and specific humidity  $q$  (2 m above ground) are monthly means, while monthly data of  $P$ , which comprises both  
rainfall  $P_{rain}$  and snowfall  $P_{snow}$ , and  $ET$  are monthly sums. Monthly values for  $\Delta S$  were computed from monthly values of  $P$   
and  $ET$  by applying Eq. (2). Data were further aggregated to annual means and sums for each hydrological year, and to mean  
monthly and annual values for the 14-year study period for each grid point of the HAR V1 10 km data set. Data were also  
70 spatially averaged for the entire Qaidam basin (2543 grid points in the HAR V1 10 km domain).

## 2.2 Meteorological data from the Global Summary of the Day

The National Centers for Environmental Information (formerly known as National Climatic Data Center) of the National  
Oceanic and Atmospheric Administration (NOAA) provide the Global Summary of the Day (GSOD), which is a collection of  
meteorological data from numerous weather stations all over the world. Eight GSOD stations providing valid data for the entire  
75 study period are located within or nearby the Qaidam basin as shown in Fig. 1.

## 2.3 Data on actual evapotranspiration

A data set of annual  $ET$  values for the Qaidam basin and eight hydrological subregions covering the time period from 2001 to  
2011 (Jin et al., 2013) was used in this study for assessing the results based on the HAR V1 10 km data set. The data set was  
derived from various data sources, especially from space-borne remote sensing data from the Moderate Resolution Imaging  
80 Spectroradiometer MODIS, by applying the Surface Energy Balance System (SEBS) algorithm (Su, 2002).

## 2.4 Statistics

Regression analyses as performed in this study are simple linear regressions and one multiple linear regression using the  
ordinary least squares method. Simple linear regressions, in which altitude  $h$  was used to as predictor variable  $x$ , were  
performed both by using  $x = h$  directly (in m a.s.l.), and by  $x = e^{h^*}$ , where  $\langle h^* = h/h_{scl} (h_{scl} = 1000 \text{ m})$ . The respective result  
85 with the highest effect size is shown in each panel of Fig. 3. Probability values  $p$  for significance testing of the regression  
results were computed from double-sided  $t$ -tests. Statistically significant results are assumed for  $p < 0.05$ . The effect size of  
the regressions is specified by the coefficient of determination  $r^2$ , which is the fraction of variance in the dependent variable  $y$   
that is explained by the linear model of the predictor variable(s)  $x$ . The effect size is further specified by the adjusted  $r^2$  ( $r^2_{adj}$ ):  
$$r^2_{adj} = 1 - (1 - r^2) \cdot (N - 1) / (N - k - 1), \quad \text{Eq. (3)}$$

90 where  $N$  is the number of observations (i.e., years;  $N = 14$ ), while  $k$  is the number of predictor variables.



### 3 Results

Table 1 lists mean monthly and annual values for the water balance components and their climate drivers, while Fig. 2 presents time series of the annual values of  $P$ ,  $ET$ , and  $\Delta S$  for the 14 years covered by this study. The results show that the Qaidam basin's water balance is nearly zero ( $\Delta S = -14 \pm 34$  mm/a) under present climate conditions. From 2005 to 2012, all years except 95 2011 show above-average annual values for the water balance due to increased annual precipitation. Rainfall is the main driver of interannual variability of both precipitation and water balance, while snowfall and actual evapotranspiration are less variable. The first year (2001) was the one with the by far most negative water balance ( $\Delta S = -94$  mm/a), and was also the coldest ( $T = -1.6$  °C) and driest ( $q = 2.2$  g/kg) year, and received the lowest amount of precipitation ( $P = 122$  mm/a), rainfall ( $P_{rain} = 45$  mm/a), and snowfall ( $P_{snow} = 77$  mm/a) (see Tables S1-S7 in the Supplement for monthly and annual values for 100 each quantity and year).

Mean monthly values for the quantities shown in Table 1 illustrate strong differences in their seasonality. While  $T$ ,  $q$ ,  $P$ ,  $P_{rain}$ ,  $P_{snow}$ , and to a lesser extent also  $ET$ , show strong variations over the year with slightly displaced winter minima and summer maxima,  $\Delta S$  is less variable during the course of the year. This indicates complex interdependencies between the climate drivers air temperature and specific humidity of the water balance components, which lead to partial compensatory effects. 105 Concurrence of the summer maxima of air temperature and precipitation in July leads to a shift of the maximum of snowfall to May, since higher air temperatures during summer reduce the fraction of precipitation falling as snow. The cold months are connected with slightly negative water balance due to sublimation of snow exceeding snowfall. The concurrently higher values of precipitation and actual evapotranspiration during summer mostly compensate each other such that water balance is only slightly positive during early summer. In August water balance even shows small water losses since precipitation decreases 110 faster than actual evapotranspiration.

Altitude dependencies of the water balance components and their climate drivers are presented in Fig. 3. While  $T$ ,  $P$ ,  $P_{snow}$ , and  $\Delta S$  show strong correlations with altitude  $h$  within the Qaidam basin,  $ET$  is only weakly correlated with  $h$ , and  $q$  is not dependent on  $h$ . At altitudes of 4000 m a.s.l. and higher, water balance becomes positive on average, and none of the HAR V1 10 km grid points shows negative values above 4700 m a.s.l., which demonstrates the importance of high mountains as water towers 115 (Xu et al., 2008) for the hydrology of a basin, especially under arid climates like those in the desert zones of High Asia.

Fig. 3 illustrates that the air over the lakes (ten grid points in the HAR V1 10 km data set) is generally warmer and less dry than over land, which is the result of high actual evapotranspiration due to lake evaporation. Although there are a few low-lying areas with very high actual evapotranspiration, the majority of land areas shows increasing actual evapotranspiration with altitude, while air temperature strongly decreases with altitude (following the mean annual moist-adiabatic lapse rate). 120 This indicates that abundance of water but not available energy is the main limiting factor for actual evapotranspiration in the Qaidam basin. In fact, the areas showing high actual evapotranspiration are mainly saline lakes that are not indicated as lakes in the HAR V1 10 km data set, such that water is available for actual evapotranspiration. Lakes tend to suppress rain- and snowfall such that their values are markedly lower over lakes. In consequence, most lakes (seven of ten grid points) show



strongly negative water balance. Further details and maps of the spatial patterns of the water balance components and their  
125 climate drivers are presented in Fig. S1 to S7 in the Supplement.

Fig. 4 presents results of simple linear regression analyses between annual values of the quantities for the entire Qaidam basin  
for the 14 hydrological years, which reveal that annual variability of water balance is driven by precipitation but not by actual  
evapotranspiration. Both precipitation and water balance are themselves driven by air temperature and specific humidity, the  
latter showing much stronger effect sizes in the simple linear regressions.

130 Since air temperature and specific humidity are themselves correlated ( $r^2 = 0.571$ ;  $r^2_{adj} = 0.535$ ;  $p < 0.01$ ; see Figure S8 in the  
Supplement), the problem of multicollinearity of the two climate drivers was addressed in this study by an additional multiple  
linear regression, in which both  $T$  and  $q$  serve as predictor variables, while  $\Delta S$  is the dependent variable. Both predictors  
together explain more than 85 % of the variance in  $\Delta S$  ( $r^2 = 0.852$ ;  $r^2_{adj} = 0.825$ ;  $p < 0.001$ ). However, the analysis revealed  
that the contribution of air temperature to the variance in water balance is not significant. Air temperature alone uniquely  
135 explains only 0.25 % ( $p_T = 0.67$ ) of the variance in water balance, while the unique variance explanation by specific humidity  
is 31.96 % ( $p_q < 0.001$ ). The combined effect of air temperature and specific humidity explains 52.97 %. Thus, the simple  
linear regression between specific humidity and water balance as shown in Fig. 3 contains both the direct and indirect effects  
of variations in specific humidity on water balance.

The results show that a change in mean annual specific humidity of 1.0 g/kg would lead to an estimated change in mean annual  
140 water balance of 131 mm/a. Since the standard error of the estimate is 14.0 mm/a, even a slight change in mean annual specific  
humidity of e.g. 0.2 g/kg would have a strong, significant effect such that the water balance of the Qaidam basin would become  
positive.

#### 4 Discussion

Physical consistency of the results obtained from the HAR V1 data set is ensured by the fact that the WRF model is physically  
145 based, and HAR V1 data have been comprehensively analysed, particularly with respect to precipitation and atmospheric water  
transport (Pritchard et al., 2019; Maussion et al., 2011, 2014; Curio et al., 2015). HAR V1 data have been successfully utilised  
for e.g. studying glacier mass balance on the Tibetan Plateau (Mölg et al., 2014), in which independent data sets from global  
reanalysis data and field measurements have also been included to ensure validity of the results. Pritchard et al. (2019) showed  
for the upper Indus basin that the HAR V1 10 km data set is particularly applicable in studies on water availability.

150 Since the HAR V1 data set, as any data set, comes with errors and uncertainties, the question arises how they would influence  
the results of the study. Fig. 3 illustrates that at six of the eight GSOD stations within or nearby the Qaidam basin the HAR V1  
precipitation data are well according to the measurements, while at two GSOD stations precipitation might be slightly  
underestimated by the HAR V1 data. A comparison of HAR V1 10 km results for actual evapotranspiration with those from  
the SEBS-based study by Jin et al. (2013) indicates higher actual evapotranspiration in the HAR V1 data. During the calendar  
155 years from 2005 to 2011, mean annual actual evapotranspiration is 218 mm/a in the HAR V1 data, while SEBS data show 153



mm/a. Both annual time series are well correlated during this time period ( $r^2 = 0.733$ ;  $r^2_{adj} = 0.679$ ;  $p < 0.05$ ; see Fig. S9 and Table S8 in the Supplement). SEBS shows inconsistent, even lower actual evapotranspiration values during the calendar years 2001 to 2004 (HAR V1:  $ET = 202$  mm/a; SEBS:  $ET = 77$  mm/a; see Table S8 in the Supplement). These findings reveal that there is no evidence that the HAR V1 data set would overestimate the water balance of the Qaidam basin. On the contrary, if  
160 SEBS actual evapotranspiration would be considered to be more accurate than HAR V1 data, then water balance would have been positive throughout all years.

The results of this study are in line with results from other studies. A number of studies (Liu and Chen, 2000; Kang et al., 2010; Li et al., 2010; Zhang et al., 2013b) revealed that the TP experiences general, but spatially and temporally varying trends to higher air temperatures, increasing humidity, and precipitation, which are also found in the Qaidam basin (Whang et al.,  
165 2014). The regions in the Qinghai province, to which the Qaidam basin belongs, show trends to warmer and wetter climates while those regions belonging to Tibet tend to warmer but dryer climates (Zhang et al., 2013b). Several studies (Zhang et al., 2011; Zhang et al., 2013a; Lei et al., 2014; Zhang et al., 2017; Li et al., 2019) reported on rising lake levels and expanding lake areas on the TP. Besides enhanced glacier melt, increasing precipitation is regarded as main driver of rising lake levels (Zhang et al., 2013a; Lei et al., 2014; Zhang et al., 2017). The total lake area in the Qaidam basin has increased from 994 km<sup>2</sup>  
170 in the 1960s to 1046 km<sup>2</sup> in 2014 (Wan et al., 2016), and the number of lakes has increased (Li et al., 2019) by 18 from 1977 to 2015. Increased water storage in the Qaidam basin does not only affect lakes but also groundwater reservoirs. Jiao et al. (2015) showed for the Qaidam basin that aquifers were recharged between 2003 and 2012 due to changes in terrestrial water storage of 20.6 km<sup>3</sup>, which is equivalent to a slightly positive mean annual water balance of 8 mm/a, while the mean value from the HAR V1 10 km data set for the corresponding time period is only slightly lower and amounts to 0 mm/a.

175 During the mid-Pliocene, climates have been generally warmer and less dry (or wetter) than today in many regions of the world (Haywood et al., 2013, 2016). The studies of Zhang et al. (2013c) and Mutz et al. (2018) provide quantitative estimates of mid-Pliocene changes in mean annual air temperature and precipitation with respect to preindustrial climates from various global paleoclimate simulations. The study of Zhang et al. (2013c) is based on a multi-model ensemble, which showed approx. 2 to 4 K higher mean annual air temperature in the Qaidam basin during the mid-Pliocene as inferred from their Fig. 6. The  
180 same Fig. 6 indicates 100 to 300 mm/a higher values for mean annual precipitation. The study of Mutz et al. (2018) is based on simulations by a single global model, showing 2 to 6 K higher mean annual air temperature in the high mountains, while it was approx. 2 to 4 K cooler in the lower parts of the Qaidam basin as inferred from their Fig. 4. Mean annual precipitation was approx. 100 to 300 mm/a higher as shown in the same Fig. 4. Both studies did not present data on differences between preindustrial and present times. Nevertheless, the values for mean annual air temperature and precipitation as presented by  
185 Fig. 4 in Mutz et al. (2018) are generally comparable to those from the HAR V1 10 km data set. Thus, present mean annual air temperature is assumed to be slightly higher (about 1 K) than during preindustrial times, such that changes in air temperature between the mid-Pliocene and present times are slightly lower but still positive (at least 1 K higher than today). Analogously, changes in precipitation are assumed to follow the same pattern (at least 50 mm/a higher than today).



190 Table 2 presents estimates for mean annual changes in the water balance of the Qaidam basin due to climate changes with respect to present conditions. The first three rows (marked in red) indicate changes in  $q$ ,  $P$ , and  $\Delta S = P - ET$  for estimates of minimum and maximum changes in  $T$ . As conservative estimates, the minimum and maximum changes in air temperature were set to 1 K and 2 K, respectively, which can be used as estimates for the air temperature range representing both mid-Pliocene climates and those projected for the end of the 21st century (Burke et al., 2018; Gu et al., 2018; Hui et al., 2018). Applying the results from the simple linear regressions (Table 2), the estimated changes in precipitation due to changes in air  
195 temperature would be 52 to 105 mm/a, which are compatible with the values modelled for the mid-Pliocene by Zhang et al. (2013c) and by Mutz et al. (2018). The mean change in water balance as inferred from the changes in air temperature would lead to a positive mean annual water balance of 49 mm/a.

Based on the same estimates for changes in air temperature, the resulting changes in specific humidity would be between 0.3 and 0.6 g/kg. Applying the sensitivities of precipitation and water balance with respect to changes in specific humidity (fourth  
200 and fifth row in Table 2; marked in blue), the resulting changes in precipitation and water balance would be almost identical to those directly estimated from the changes in air temperature.

The sixth row of Table 2 (marked in black) shows the results for changes in water balance for given changes in precipitation. The minimum and maximum values for the changes in precipitation (50 to 100 mm/a) are conservative estimates but also compatible with the studies of Zhang et al. (2013c) and Mutz et al. (2018). The mean change in water balance as inferred from  
205 the changes in precipitation would lead to a positive mean annual water balance of 40 mm/a.

Warmer and less dry conditions in the Qaidam basin are also confirmed from geological evidence (Miao et al., 2013; Wu et al., 2011; Cai et al., 2012). The very high sensitivity of water balance to changes in air temperature and specific humidity as revealed in this study would explain that even slightly warmer and less dry climates would result in positive long-term mean annual water balance such that the mega-lake system would have been able to exist in this still very dry region for long time.  
210 Since the high mountain ranges are of utmost importance in this respect, the question arises, how different the paleogeographic situation has been in the Qaidam basin as compared with today. Although the details of tectonics are not yet finally clarified, and vertical movements of the lithosphere have certainly influenced the basin's orography (Fang et al., 2007), the results of this study are considered to be generally applicable to the mid-Pliocene, since the paleogeographic situation of this epoch has been similar to the present (Dowsett et al., 2010). If altitudes of the high mountain ranges in the Qaidam basin would have  
215 been a few hundredths meters lower than today as indicated by Fang et al. (2007), then the negative effect of lower altitudes on water balance would be accompanied by the counteracting effect that blocking of humid air masses by the high mountain ranges in the fringes of the Qaidam basin would have been less strong, a fact also studied for the entire TP (Broccoli and Manabe, 1992). This statement is also justified by the results obtained by applying the same methodology as used in this study to the HAR V1 data set for the 30 km domain (see Table S9, Figures S10 and S11 in the Supplement). Due to the coarser  
220 model grid, the altitudes of the highest mountains are lower in the 30 km grid ( $h_{max} = 5.136$  m a.s.l.) than in the 10 km grid ( $h_{max} = 5.433$  m a.s.l.), and the mean annual water balance rises from -14 mm/a (10 km grid) to 3 mm/a (30 km grid).



## 5 Conclusions

Global climate change as projected for the future and its consequences for the regional climates of China (Burke et al., 2018; Gu et al., 2018; Hui et al., 2018) could lead to strengthening of the East Asian Summer Monsoon (Wang et al., 2008), which  
225 could also affect the Qaidam basin such that both specific humidity and precipitation would increase. This would then lead to continued recharge of groundwater reservoirs and, at a later stage, to rising lake levels or formation of new lakes. In a long-term perspective, even the Qaidam mega-lake system may be restored. Assuming a slightly positive long-term mean annual water balance of 40 mm/a as discussed above, lake water levels would rise by 400 m averaged over the entire Qaidam basin within only 10 ka, which is, in a geological perspective, a very short time period. Since water would preferentially accumulate  
230 in the low-lying areas, the effect would be even stronger in those areas, which have formerly been part of the Qaidam mega-lake system.

Future research could target on acquisition of additional or improved spatially distributed data sets for water balance components and climate drivers at even higher spatial resolution to capture the details of the high mountain topography of the Qaidam basin, and for longer time periods to improve assessments of environmental changes related to changes in water  
235 balance. The new global ERA5 reanalysis data set, as well as the transferability of the methods applied in this study to other regions offer new options in this respect. Other lines of research could focus on dynamical downscaling of paleoclimate simulations for Pliocene time slices or global climate projections for the future. Both kind of data sets are, in general, spatially too coarse to fully resolve atmospheric processes like orographically induced precipitation or actual evapotranspiration in high mountain ranges (Gu et al., 2018), such that regional water balance computations based on coarse data would, most likely,  
240 come with high uncertainties. Thus, dynamical downscaling of global atmospheric data is regarded to be essential.

Dynamical downscaling could also be used to study changes in the statistical relations as revealed in this study by artificially modified (paleo-)geographies. Since lakes tend to reduce precipitation while concurrently showing high actual evaporation, there should be an upper limit for lake growth, which is, however, not yet known. On the other hand, it is theoretically also possible that a mega-lake system effectively recycles its own water, i.e., that atmospheric moisture stemming from lake  
245 evaporation precipitates within the basin's catchment area. Water recycling is highly important for the entire TP (Curio et al., 2015), and might also play an important, yet unknown role for the Qaidam basin's water balance.

250 **Data availability.** The HAR V1 data set is freely availability at <http://www.klima.tu-berlin.de/HAR>.

**Supplement.** The supplement related to this article is available online at:

**Author contribution.** Dieter Scherer carried out the analyses and wrote the paper.





255

**Competing interests.** The author declares that he has no conflict of interest.

**Acknowledgments.** I would like to thank Fabien Maussion (University of Innsbruck, Austria) and Julia Curio (University of Reading, United Kingdom) for their participation in the development of the High Asia Refined analysis data set (HAR V1), to  
260 Erwin Appel, Svetlana Botsyun, Todd Ehlers, Sebastian Mutz (University of Tübingen), and to Marco Otto, Vanessa Tolksdorf, and Xun Wang (Technische Universität Berlin, Germany) for collaboration and discussions within the Q-TiP project.

**Financial support.** This work was supported by the German Research Foundation (DFG) Priority Programme 1372, “Tibetan  
265 Plateau: Formation - Climate - Ecosystems” within the DynRG-TiP project “Dynamic Response of Glaciers on the Tibetan Plateau to Climate Change” (codes SCHE 750/4-1, SCHE 750/4-2, SCHE 750/4-3), and by the German Federal Ministry of Education and Research (BMBF) Programmes “Central Asia - Monsoon Dynamics and Geo-Ecosystems” (CAME) within the WET project “Variability and Trends in Water Balance Components of Benchmark Drainage Basins on the Tibetan Plateau” (code 03G0804A), and the follow-on Programme CAME II within the Q-TiP project “Quaternary Tipping Points of Lake  
270 Systems in the Arid Zone of Central Asia” (code 03G08063C).

## References

- An, Z., Kutzbach, J. E., Prell, W. L., and Porters, S. C.: Evolution of Asian monsoons and phased uplift of the Himalaya-Tibetan plateau since Late Miocene times, *Nature*, 411, 62-66, 2001.
- Broccoli, A.J. and Manabe, S.: The Effects of Orography on Midlatitude Northern Hemisphere Dry Climates, *J. Clim.*, 5, 1181-  
275 1201, 1992.
- Burke, K. D., Williams, J. W., Chandler, M. A., Haywood, A. M., Lunt, D. J., and Otto-Bliesner, B. L.: Pliocene and Eocene provide best analogs for near-future climates, *PNAS*, 115, 13288-13293, 2018.
- Cai, M., Fang, X., Wu, F., Miao, Y., and Appel, E.: Pliocene–Pleistocene stepwise drying of Central Asia: Evidence from paleomagnetism and sporopollen record of the deep borehole SG-3 in the western Qaidam Basin, NE Tibetan Plateau, *Global  
280 Planet. Change*, 94-95, 72-81, 2012.
- Chen, K. and Bowler, J. M.: Late pleistocene evolution of salt lakes in the Qaidam basin, Qinghai province, China, *Paleogeogr. Paleoclimatol. Paleoecol.*, 54, 87-104, 1986.
- Curio, J., Maussion, F., and Scherer, D.: A 12-year high-resolution climatology of atmospheric water transport over the Tibetan Plateau, *Earth Syst. Dynam.*, 6, 109-124, 2015.
- 285 Dowsett, H., Robinson, M., Haywood, A., Salzmann, U., Hill, D., Sohl, L., Chandler, M., Williams, M., Foley, K., and Stoll, D.: The PRISM3D paleoenvironmental reconstruction, *Stratigraphy*, 7, 123-139, 2010.



- Fang, X., Zhang, W., Meng, Q., Gao, J., Wang, X., King, J., Song, C., Dai, S., and Miao, Y.: High-resolution magnetostratigraphy of the Neogene Huaitoutala section in the eastern Qaidam Basin on the NE Tibetan Plateau, Qinghai Province, China and its implication on tectonic uplift of the NE Tibetan Plateau, *Earth and Planetary Science Letters*, 258, 293-306, 2007.
- Greve, P., Gudmundsson, L., and Seneviratne, S. I.: Regional scaling of annual mean precipitation and water availability with global temperature change, *Earth Syst. Dynam.*, 9, 227-240, 2018.
- Gu, H., Yu, Z., Yang, C., Ju, Q., Yang, T., and Zhang, D.: High-resolution ensemble projections and uncertainty assessment of regional climate change over China in CORDEX East Asia, *Hydrol. Earth Syst. Sci.*, 22, 3087-3103, 2018.
- Haywood, A. M. et al.: Large-scale features of Pliocene climate: results from the Pliocene Model Intercomparison Project, *Clim. Past*, 9, 191-209, 2013.
- Haywood, A. M., Dowsett, H. J., and Dolan, A. M.: Integrating geological archives and climate models for the mid-Pliocene warm period, *Nature Communications*, 7, 10646, 2016.
- Heermance, R. V., Pullen, A., Kapp, P., Garzzone, C. N., Bogue, S., Ding, L., and Song, P.: Climatic and tectonic controls on sedimentation and erosion during the Pliocene-Quaternary in the Qaidam Basin (China), *GSA Bulletin*, 125, 833-856, 2013.
- Huang, Q., Ku, T.-L., and Phillips, F. M.: Evolutionary characteristics of lakes and palaeoclimatic undulations in the Qaidam Basin, China, *Chin. J. Oceanol. Limnol.*, 11, 34-45, 1993.
- Hui, P., Tang, J., Wang, S., Niu, X., Zong, P., and Dong, X.: Climate change projections over China using regional climate models forced by two CMIP5 global models. Part II: projections of future climate, *Int. J. Climatol.*, 38, e78-e94, 2018.
- Jiao, J.J., Zhang, X., Liu, Y., and Kuang, X.: Increased water storage in the Qaidam Basin, the north Tibet Plateau from GRACE gravity data, *PLoS ONE*, 10, e0141442, 2015.
- Jin, X., Guo, R., and Xia, W.: Distribution of actual evapotranspiration over Qaidam Basin, an arid area in China, *Remote Sens.*, 5, 6976-6996, 2013.
- Kang, S., Xu, Y., You, Q., Flügel, W.-A., Pepin, N., and Yao, T.: Review of climate and cryospheric change in the Tibetan Plateau, *Environ. Res. Lett.*, 5, 015101, 2010.
- Lehner, B. and Grill G.: Global river hydrography and network routing: baseline data and new approaches to study the world's large river systems, *Hydrological Processes*, 27, 2171-2186, 2013. Data is available at [www.hydrosheds.org](http://www.hydrosheds.org).
- Lei, Y., Yang, K., Wang, B., Sheng, Y., Bird, B. W., Zhang, G., and Tian, L.: Response of inland lake dynamics over the Tibetan Plateau to climate change, *Clim. Chang.*, 125, 281-290, 2014.
- Li, L., Yang, S., Wang, Z., Zhu, X., and Tang, H.: Evidence of warming and wetting climate over the Qinghai-Tibet Plateau, Arctic, Antarctic, and Alpine Research, 42, 449-457, 2010.
- Li, H., Mao, D., Li, X., Wang, Z., and Wang, C.: Monitoring 40-Year Lake Area Changes of the Qaidam Basin, Tibetan Plateau, Using Landsat Time Series, *Remote Sens.*, 11, 343, 2019.
- Liu, X. and Chen, B.: Climatic warming in the Tibetan Plateau during recent decades, *Int. J. Climatol.* 20, 1729-1742, 2000.



- 320 Madsen, D. B., Lai, Z., Sun, Y., Rhode, D., Liu, X., and Brantingham, P. J.: Late Quaternary Qaidam lake histories and implications for an MIS 3 “Greatest Lakes” period in northwest China, *J. Paleolimnol.*, 51, 161-177, 2014.
- Maussion, F., Scherer, D., Finkelnburg, R., Richters, J., Yang, W., and Yao, T.: WRF simulation of a precipitation event over the Tibetan Plateau, China - an assessment using remote sensing and ground observations, *Hydrol. Earth Syst. Sci.*, 15, 1795-1817, 2011.
- 325 Maussion, F., Scherer, D., Mölg, T., Collier, E., Curio, J., and Finkelnburg, R.: Precipitation seasonality and variability over the Tibetan Plateau as resolved by the High Asia Reanalysis, *J. Clim.*, 27, 1910-1927, 2014.
- Miao, Y. F., Fang, X. M., Wu, F. L., Cai, M. T., Song, C. H., Meng, Q. Q., and Xu, L.: Late Cenozoic continuous aridification in the western Qaidam Basin: evidence from sporopollen records, *Clim. Past*, 9, 1863-1877, 2013.
- Mischke, S., Sun, Z., Herzsuh, U., Qiao, Z., and Sun, N.: An ostracod-inferred large Middle Pleistocene freshwater lake in the presently hyper-arid Qaidam Basin (NW China), *Quat. Int.*, 218, 74-85, 2010.
- 330 Mölg, T., Maussion, F., and Scherer, D.: Mid-latitude westerlies as a driver of glacier variability in monsoonal High Asia, *Nature Climate Change*, 4, 68-73, 2014.
- Morrow, E., Mitrovica, J. X., and Fotopoulos, G.: Water storage, net precipitation, and evapotranspiration in the Mackenzie River Basin from October 2002 to September 2009 inferred from GRACE satellite gravity data, *J. Hydrometeor.*, 12, 467-473, 335 2011.
- Mutz, S. G., Ehlers, T. A., Werner, M., Lohmann, G., Stepanek, C., and Li, J.: Estimates of late Cenozoic climate change relevant to Earth surface processes in tectonically active orogens, *Earth Surface Dynamics*, 6, 271-301, 2018.
- Pritchard, D. M., Forsythe, N., Fowler, H. J., O’Donnell, G. M., and Li, X.: Evaluation of Upper Indus near-surface climate representation by WRF in the High Asia Refined Analysis, *J. Hydrometeor.*, 20, 467-487, 2019.
- 340 Su, Z.: The Surface Energy Balance System (SEBS) for estimation of turbulent heat fluxes, *Hydrol. Earth Syst. Sci.*, 6, 85-99, 2002.
- Wan, W., Long, D., Hong, Y., Ma, Y., Yuan, Y., Xiao, P., Duan, H., Han, Z., and Gu, X.: A lake data set for the Tibetan Plateau from the 1960s, 2005, and 2014, *Scientific data*, 3, 160039, 2016.
- Wang, B., Bao, Q., Hoskins, B., Wu, G., and Liu, Y.: Tibetan Plateau warming and precipitation changes in East Asia, 345 *Geophys. Res. Lett.*, 35, L14702, 2008.
- Wang, J. Y., Fang, X., Appel, E., and Song, C.: Pliocene-Pleistocene climate change at the NE Tibetan Plateau deduced from lithofacies variation in the drill core SG-1, western Qaidam Basin, *J. Sedimentary Res.*, 82, 933-952, 2012.
- Wang, X., Yang, M., Liang, X., Pang, G., Wan, G., Chen, X., and Luo, X.: The dramatic climate warming in the Qaidam Basin, northeastern Tibetan Plateau, during 1961 – 2010, *Int. J. Climatol.*, 34, 1524-1537, 2014.
- 350 Wu, F. L., Fang, X. M., Herrmann, M., Mosbrugger, V., and Miao, Y. F.: Extended drought in the interior of Central Asia since the Pliocene reconstructed from sporopollen records, *Global Planet. Change*, 76, 16-21, 2011.
- Xu, X., Lu, C., Shi, X., and Gao, S.: World water tower: An atmospheric perspective, *Geophys. Res. Lett.*, 35, L20815, 2008.



- Yu, S.-Y., Colman, S. M., and Lai, Z.-P.: Late-Quaternary history of ‘great lakes’ on the Tibetan Plateau and paleoclimatic implications - A review, *Boreas*, 48, 1-19, 2019.
- 355 Zhang, G., Xie, H., Kang, S., Yi, D., and Ackley, S. F.: Monitoring lake level changes on the Tibetan Plateau using ICESat altimetry data (2003-2009), *Remote Sens. Environ.*, 115, 1733-1742, 2011.
- Zhang, G., Yao, T., Xie, H., Kang, S., and Lei, Y.: Increased mass over the Tibetan Plateau: From lakes or glaciers? *Geophys. Res. Lett.*, 40, 2125-2130, 2013a.
- Zhang, L., Guo, H., Ji, L., Wang, C., Yan, D., Li, B., and Li J.: Vegetation greenness trend (2000 to 2009) and the climate  
360 controls in the Qinghai-Tibetan Plateau, *J. Appl. Rem. Sens.*, 7, 073572, 2013b.
- Zhang, R., Yan, Q., Zhang, Z. S., Jiang, D., Otto-Bliesner, B. L., Haywood, A. M., Hill, D. J., Dolan, A. M., Stepanek, C., Lohmann, G., Contoux, C., Bragg, F., Chan, W. L., Chandler, M. A., Jost, A., Kamae, Y., Abe-Ouchi, A., Ramstein, G., Rosenbloom, N. A., Sohl, L., and Ueda, H.: Mid-Pliocene East Asian monsoon climate simulated in the PlioMIP, *Clim. Past*, 9, 2085-2099, 2013c.
- 365 Zhang, G., Yao, T., Shumm, C. K., Yi, S., Yang, K., Xie, H., Feng, W., Bolch, T., Wang, L., Behrangi, A., Zhang, H., Wang, C., Xiang, Y., and Yu, J.: Lake volume and groundwater storage variations in Tibetan Plateau's endorheic basin, *Geophys. Res. Lett.*, 44, 5550-5560, 2017.
- Zubakov, V. A. and Borzenkova, I. I.: Pliocene palaeoclimates: past climates as possible analogues of mid-twenty-first century climate, *Palaeogeogr. Palaeoclimatol. Palaeoecol.*, 65, 35-49, 1988.

370

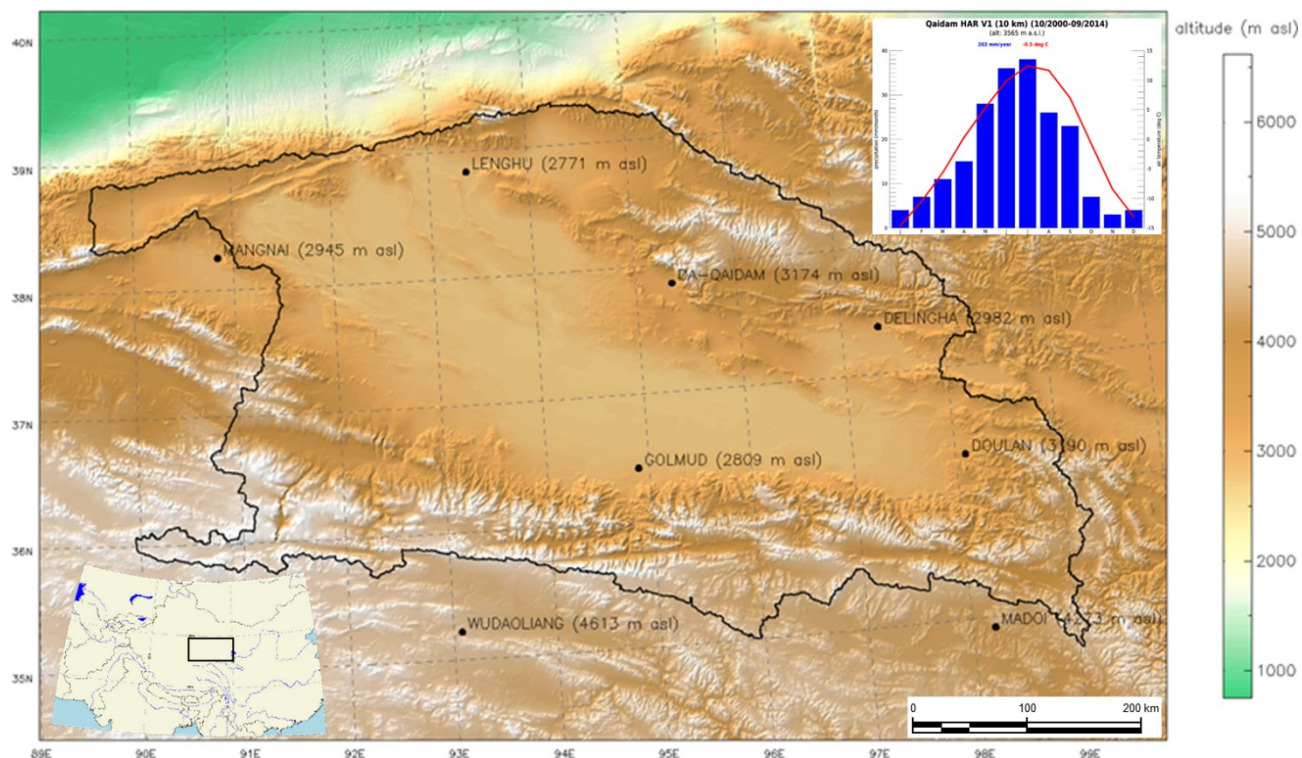
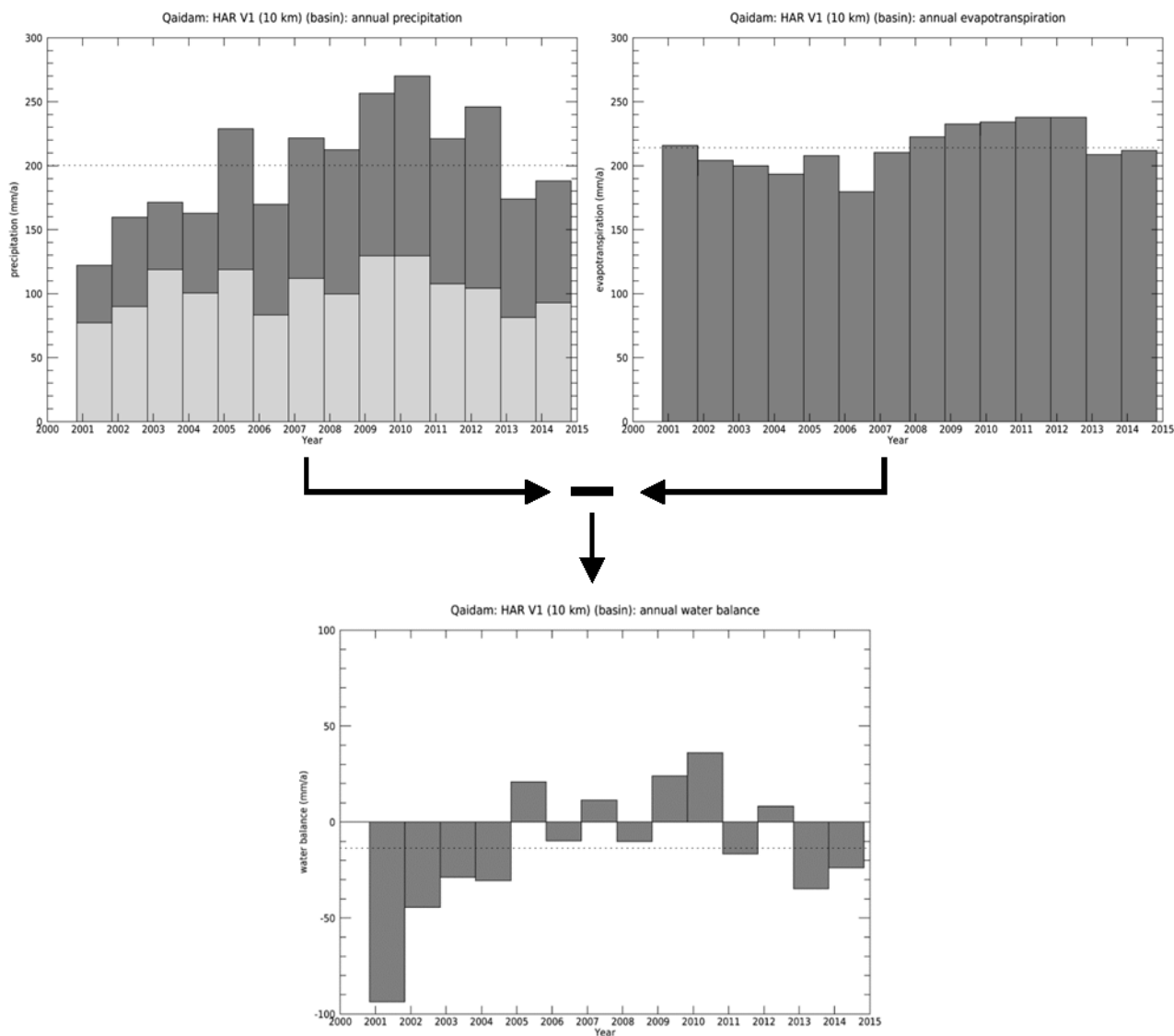
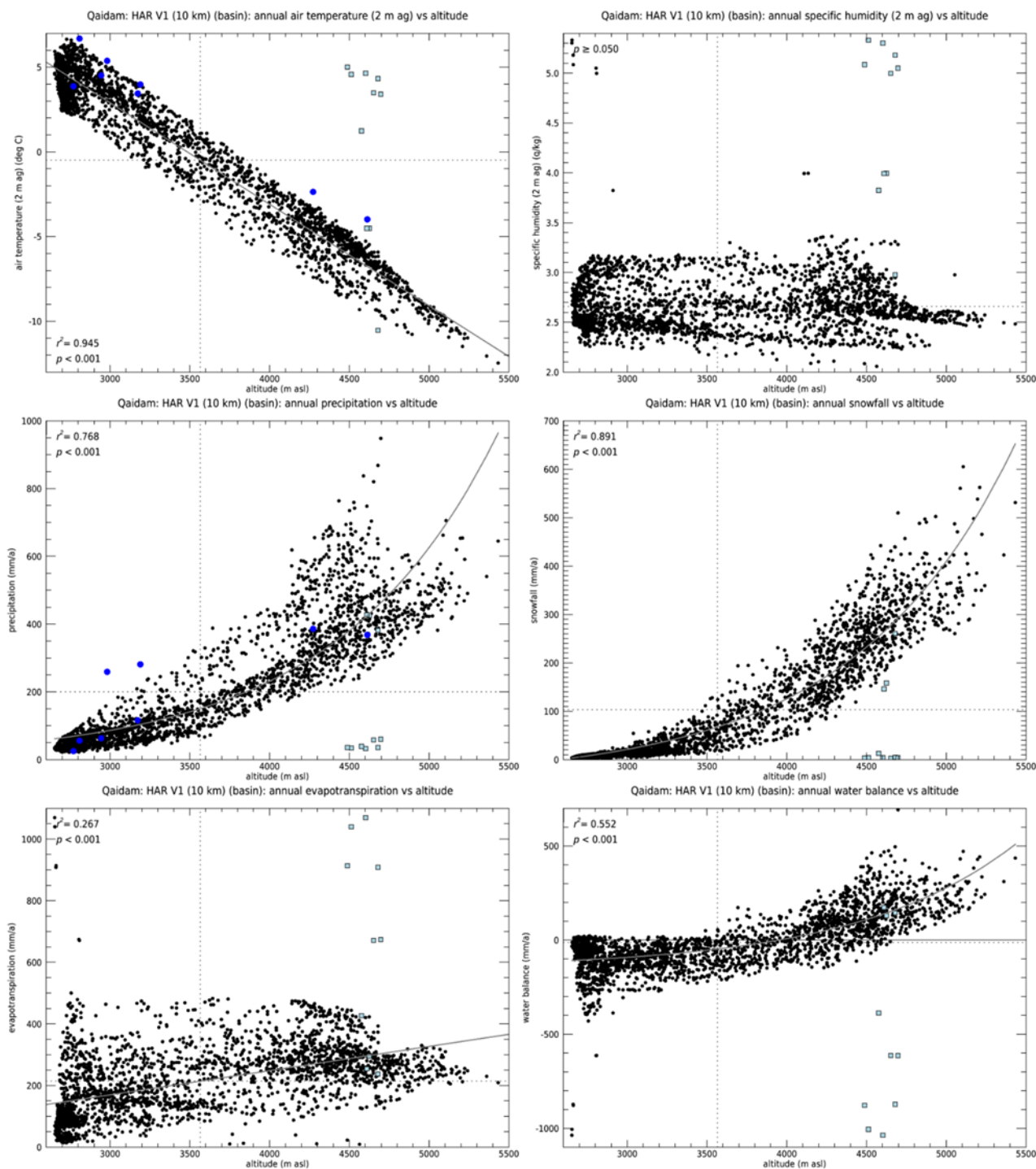


**Figure 1: Overview on the Qaidam basin, including a spatially averaged climate diagram for the Qaidam basin derived from the HAR V1 (10 km) data set for the study period of 14 hydrological years (2001-2014). Black line: boundary of the Qaidam basin (Lehner and Grill, 2013). Topographic shading is based on DEM data from the SRTM.**

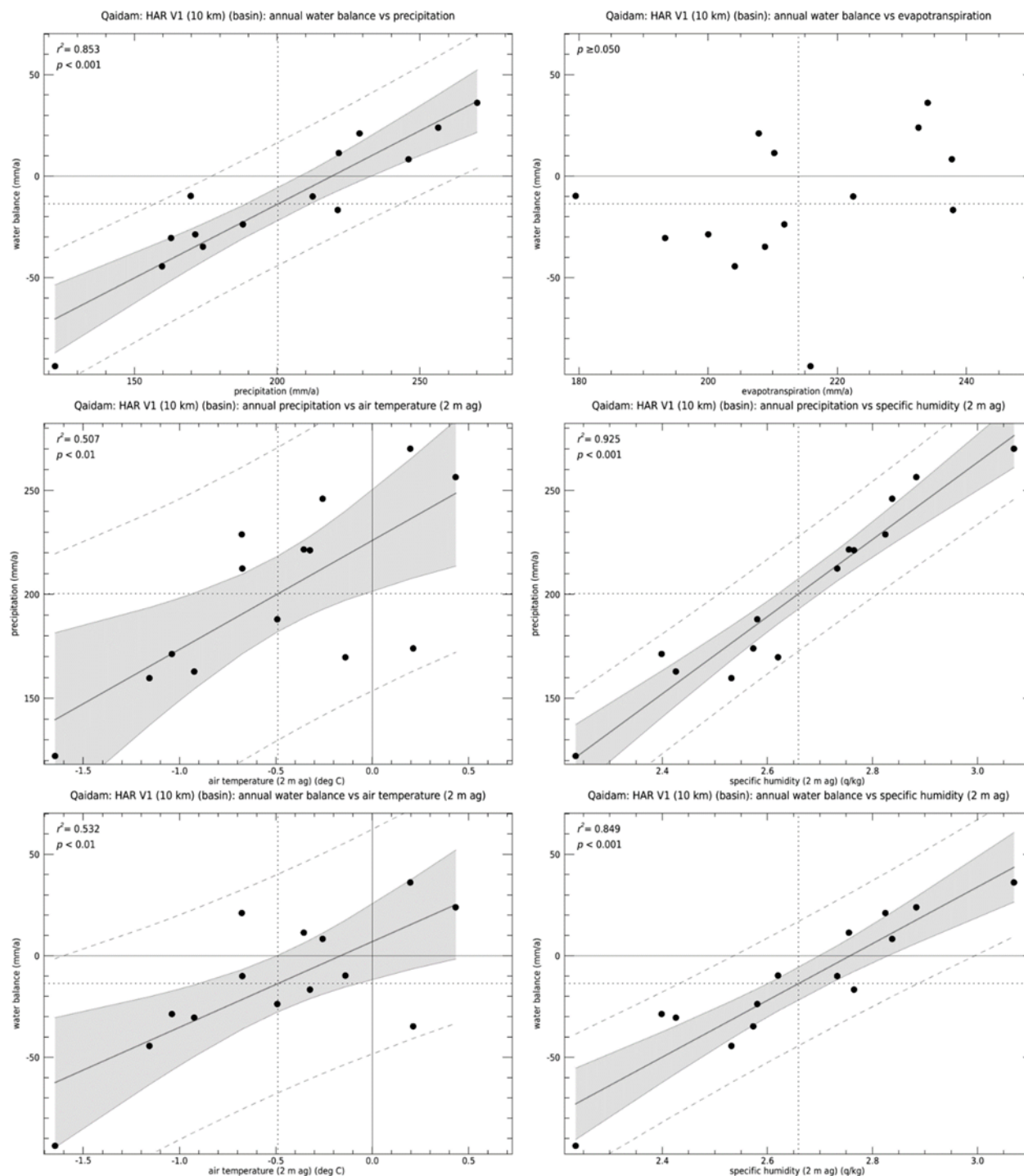


375

**Figure 2:** Annual precipitation  $P$  (upper left), actual evapotranspiration  $ET$  (upper right), and water balance  $\Delta S = P - ET$  (lower) in the Qaidam basin. Upper left: light grey bars: annual snowfall  $P_{snow}$ ; dark grey bars: annual rainfall  $P_{rain} = P - P_{snow}$ . Dotted lines: mean annual values.



380 **Figure 3:** Mean annual air temperature  $T$  (upper left), specific humidity  $q$  (upper right), precipitation  $P$  (middle left), snowfall  $P_{snow}$  (middle right), actual evapotranspiration  $ET$  (lower left), and water balance  $\Delta S = P - ET$  (lower right) versus altitude in the Qaidam basin. Black dots: terrestrial grid points; light blue squares: grid points covered by lakes in the HAR V1 (10 km) land cover data; blue dots: data from eight GSOD stations; dotted lines: mean annual values.



385 **Figure 4:** Water balance  $\Delta S = P - ET$  versus precipitation  $P$  (upper left) and actual evapotranspiration  $ET$  (upper right);  $P$  versus air temperature  $T$  (middle left) and specific humidity  $q$  (middle right);  $\Delta S$  versus  $T$  (lower left) and  $q$  (lower right) in the Qaidam basin during the hydrological years 2001 to 2014. Dotted lines: annual means; solid lines: regression lines; light grey shades: confidence intervals; dashed lines: prediction intervals.





390 **Table 1: Mean monthly and annual air temperature  $T$ , specific humidity  $q$ , precipitation  $P$ , rainfall  $P_{rain}$ , snowfall  $P_{snow}$ , actual evapotranspiration  $ET$ , and water balance  $\Delta S = P - ET$  in the Qaidam basin; sigma: standard deviations of annual values for each quantity during the 14-years study period.**

month	10	11	12	1	2	3	4	5	6	7	8	9	year	sigma
$T$ (deg C)	-0.7	-8.4	-13.1	-14.6	-10.5	-5.6	0.3	5.3	9.9	12.4	11.6	7.0	<b>-0.5</b>	0.6
$q$ (g/kg)	2.2	1.4	1.0	0.9	1.2	1.5	1.9	2.8	4.3	5.6	5.1	3.9	<b>2.7</b>	0.2
$P$ (mm)	7	3	4	4	7	11	15	28	36	38	26	23	<b>200</b>	43
$P_{rain}$ (mm)	1	0	0	0	1	1	4	9	21	30	19	12	<b>97</b>	31
$P_{snow}$ (mm)	6	3	4	4	6	10	11	19	15	8	7	11	<b>103</b>	17
$ET$ (mm)	13	8	5	5	9	15	18	25	29	34	31	21	<b>214</b>	18
$P-ET$ (mm)	-6	-4	-1	-2	-2	-4	-4	2	7	4	-5	1	<b>-14</b>	34

395 **Table 2: Estimated changes in long-term mean annual air temperature  $T$ , specific humidity  $q$ , precipitation  $P$ , and water balance  $\Delta S = P - ET$  (actual evapotranspiration) in the Qaidam basin, and resulting water balance for the mid-Pliocene or for future climates due to anthropogenic climate change. Red colours: estimates based on  $T$ ; blue colours: estimates based on  $q$ ; black colours: estimates based on  $P$ . Input values for  $T$  (magenta shades) and  $P$  (grey shades) are estimates based on the studies of Zhang et al. (2013c) and Mutz et al. (2018).**

sensitivity	value	unit	$\Delta T$		$\Delta q$		$\Delta P$		$\Delta(P-ET)$		$P-ET$			
			min	max	min	max	min	max	min	max	min	max	mean	
$\partial q / \partial T$	0.288	g/(kg·K)	1.0	2.0	0.3	0.6								
$\partial P / \partial T$	52.40	mm/(a·K)					52	105						
$\partial(P-ET) / \partial T$	42.17	mm/(a·K)							42	84	28	70	49	
$\partial P / \partial q$	185.6	mm·kg/(a·g)			0.3	0.6	53	107						
$\partial(P-ET) / \partial q$	139.7	mm·kg/(a·g)							40	81	26	67	46	
$\partial(P-ET) / \partial P$	0.725	mm/mm					50	100	36	73	22	59	40	

400